J|A|C|S COMMUNICATIONS

Published on Web 10/08/2009

# Probing Interfacial Electron Transfer in Coumarin 343 Sensitized $TiO_2$ Nanoparticles with Femtosecond Stimulated Raman

Renee R. Frontiera, Jyotishman Dasgupta, and Richard A. Mathies*

*Department of Chemistry, University of California, Berkeley, California 94720*

Received August 25, 2009; E-mail: rich@zinc.cchem.berkeley.edu

Interfacial photoinduced electron transfer reactions are of crucial importance in a multitude of chemical and physical applications, including solar energy capture and conversion devices, molecular nanoelectronics, and photocatalytic pollutant treatment.[1] However, the exact molecular mechanism of ultrafast electron transfer when there is strong electronic coupling between donor and acceptor, such as that in dye sensitized solar cells (DSSCs), is not clear.[2,3] In these systems, electron transfer occurs on the 5 femtosecond (fs) to several picosecond (ps) time scale.[4] With such rapid transfer, the donor does not have time to thermally equilibrate, as is traditionally assumed in models of electron transfer. Thus specific vibrational excitation and postexcitation nuclear motions are expected to play a significant role in the charge transfer process, preempting the conventional thermalized adiabatic ET mechanism.[5]

Here we examine the initial structural dynamics of a dye sensitizer attached to semiconducting nanoparticles before and after interfacial electron transfer, with the goal of providing insight into which vibrational modes mediate the electron transfer pathway. We also determine the localization of the hole after donation, which may affect the efficiency of unwanted back electron transfer reactions. These time dependent nuclear motions are revealed by femtosecond stimulated Raman spectroscopy (FSRS), a spectroscopic technique that provides well-resolved vibrational structural information that is not compromised by features from fluorescence or scattering.[6,7] These experiments represent an initial demonstration of the feasibility of using FSRS to obtain Raman spectra of colloidal dye sensitized nanoparticle solutions.

Coumarin 343 (C343) is an ideal system for studying electron transfer into $TiO_2$, as it is known to undergo fast electron injection[3,8−11] with ∼80−90% efficiency[8,12] according to the following scheme:

$$TiO_2{-}C343 \xrightarrow{h\nu} TiO_2{-}C343^* \xrightarrow{\text{fast ET}}$$

$$TiO_2^{\bullet-}{-}C343^{\bullet+} \xrightarrow{\text{slow recomb}} TiO_2{-}C343$$

C343 and its derivatives have been successfully used in organic dye-sensitized solar cells.[13−15] The chemical structure of C343, as well as the bathochromic shift in the absorption band upon formation of the C343−$TiO_2$ charge transfer complex, is presented in Figure 1. It is thought that the carboxyl group of C343 binds directly to titanium atoms on the surface of the nanoparticle.[2] Transient absorption in the visible[8,10] and probing the infrared conduction band of $TiO_2$[9] both indicate that electron injection from the C343 to the nanoparticle occurs in <100−180 fs. However, these techniques probe only the overlapping electronic states and are not structurally specific. Here we use two vibrational spectroscopies, resonance Raman and femtosecond stimulated Raman, to probe the structural changes of this system during and after

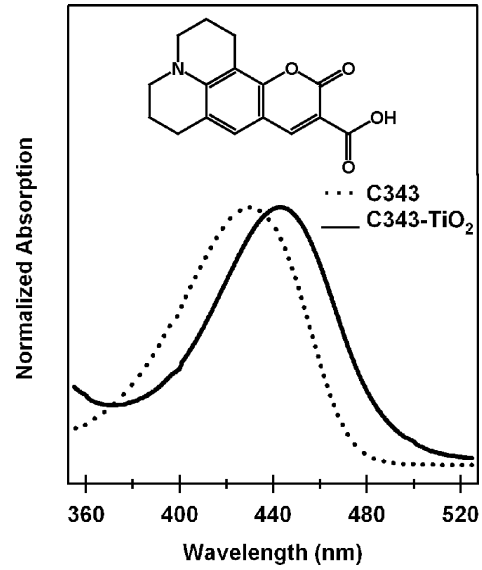


***Figure 1.*** Structure and normalized absorption spectra of Coumarin 343 in methanol (dashed) and bound to $TiO_2$ nanoparticles (solid). The shift in the absorption is due to formation of the charge-transfer complex.

interfacial electron transfer. The ground state resonance Raman spectrum gives information on the initial motions after excitation to the Franck−Condon region, and femtosecond stimulated Raman provides direct information on the structure from 50 fs to 50 ps.

To probe the Franck−Condon dynamics in the first femtoseconds following photoexcitation, we examined the resonance Raman intensities. Resonance Raman intensities give information on initial excited state dynamics by determining which vibrational motions are coupled to the electronic excitation.[16,17] Modes which are intense in the resonance Raman spectra are those which lead the geometric distortion out of the Franck−Condon region of the potential energy surface. In the C343−$TiO_2$ charge transfer system, traditional continuous wave Raman techniques are hindered by the strong fluorescence from unbound C343 molecules as well as scattering from the nanoparticles at low wavenumbers. To minimize the fluorescence and scattering background, we used stimulated resonance Raman[18] with an 800 fs Raman pump pulse at 530 nm to examine the initial excited state vibrational dynamics which contribute to the ultrafast charge transfer process in C343−$TiO_2$.

The ground state resonance Raman spectrum of C343 bound to $TiO_2$ nanoparticles is shown in Figure 2. Solutions of $TiO_2$ or C343 alone in methanol exhibit no significantly enhanced vibrational modes with 530 nm excitation. However, upon formation of the charge-transfer complex, dramatic mode enhancements at multiple wavelengths are evident, revealing modes at ∼500, 632, 784, 1366, 1471, and 1651 $cm^{-1}$ that are not seen in unbound C343 either off (Figure 2) or on (Figure S2) resonance. The character of these



10.1021/ja907188b CCC: $40.75 

ground state resonance Raman modes of the charge-transfer complex have been determined by comparison with DFT calculations at the B3LYP/6-31G level.[19] The 632 and 784 $cm^{-1}$ modes are ring breathing, 1366 $cm^{-1}$ is C−C stretching, 1471 $cm^{-1}$ is a C−C, C═C, and C−N stretching mode, and 1651 $cm^{-1}$ is a C═O stretch. The cluster of modes between 400 and 550 $cm^{-1}$ in Figure 2 are not predicted by the DFT calculation and correspond to Ti−O stretching modes.[20] Since only C343 is resonantly enhanced at this wavelength, these modes likely arise from the direct binding of the carboxylic acid foot to the nanoparticle surface, and the broad peaks result from multiple binding configurations. The presence of these modes also indicates a significant degree of orbital overlap between the dye and the nanoparticle surface.

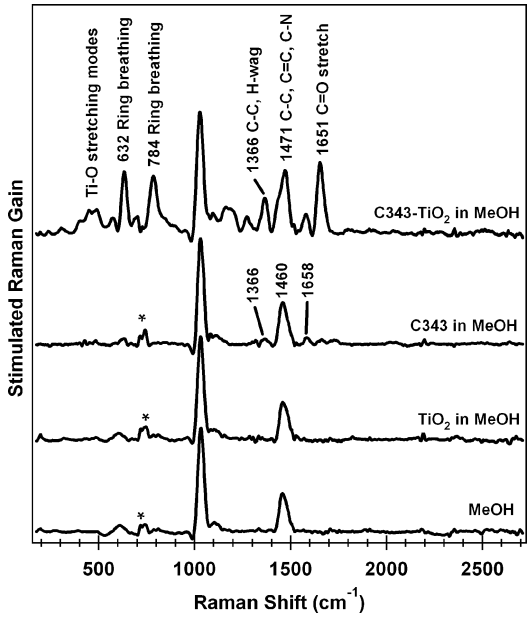


***Figure 2.*** Ground state resonance Raman spectra of the C343−$TiO_2$ charge transfer complex compared to the individual components of the solution (MeOH = methanol). Resonance enhancement of at least six modes of the C343−$TiO_2$ complex is evident. Asterisks mark detection artifacts.

The surprisingly large number of modes enhanced in the resonance Raman spectra of C343−$TiO_2$ suggest that multiple vibrational motions play an important role in the ultrafast charge-transfer process. This observation has important implications in theoretical models of electron transfer, as traditionally only one or at most two nuclear degrees of freedom are implicated in the transfer. Additionally, the modes which are most enhanced are those with greatest contributions from carbon backbone motions, such as the 632 and 784 $cm^{-1}$ ring breathing modes and the higher frequency modes at 1366 and 1471 $cm^{-1}$ which consist of predominantly carbon stretching motions. Modes involving primarily C−N stretching features, which would have indicated hole localization on the nitrogen, are not significantly enhanced. The rapid speed of electron transfer and relatively strong coupling between the dye and semiconductor indicate that enhanced modes will be ones which lead directly to electron transfer. Based on the nature of the modes observed here, it seems likely that the donated electron density comes from the delocalized pi backbone system, rather than from the nitrogen or the unconjugated rings.

We next investigated this photoinduced electron transfer with FSRS to examine the changes in vibrational structure following the charge-transfer process. FSRS is a technique which provides high resolution structural information over the course of a photochemical reaction, with simultaneous 10 $cm^{-1}$ vibrational resolution and 50−200 fs time resolution.[6] In FSRS, a femtosecond actinic pulse initiates the photochemistry, and a picosecond 800 nm Raman pump pulse and femtosecond probe pulse interrogate the time-resolved structure at various time delays. The details of the experimental setup are described elsewhere[21] (and see Supporting Information). The charge-transfer complex was photoexcited at 500 nm to avoid exciting any unbound C343 molecules.

The time-resolved vibrational spectra of the C343−$TiO_2$ system, along with the neutral ground state spectrum, are presented in Figure 3A. The time-resolved spectra are characterized by the immediate appearance of ground state radical cation peaks at 1205, 1358, and 1549 $cm^{-1}$. A comparison with the neutral ground state spectrum reveals that the doublet at 1565 and 1592 $cm^{-1}$ has downshifted to a single intense cation peak at 1549 $cm^{-1}$. The weak neutral feature at 1372 $cm^{-1}$ shifts to 1358 $cm^{-1}$, and the lower frequency 781 $cm^{-1}$ ground state mode has no corresponding features in the radical cation spectrum. A kinetic plot of the amplitude of the 1549 $cm^{-1}$ peak is shown in Figure 3B. The amplitude is fit to two exponentials convolved with the cross correlation time of 140 fs, and the dynamics of this peak fits nicely with a 120 fs risetime. The decay of this peak is characterized by a long time decay (250 ps), which is assigned to charge recombination,[9] and a 1.3 ps time constant which has not been previously observed. Additionally, we observe a 4 $cm^{-1}$ blue shift in the 1549 $cm^{-1}$ peak on the 3 ps time scale (Figure 3S) which can be assigned to vibrational cooling.

We assign the spectra that are seen at early times and persist until many picoseconds to the ground state radical cation of C343. This assignment is in agreement with previous transient absorption measurements which found a similar risetime in the growth of an absorption in the conduction band of the oxidized $TiO_2$.[9] The time-resolved vibrational spectra reveal that the structure of the radical cation does not change significantly throughout its lifetime. The vibrational frequencies and intensities of the peaks are significantly different from the neutral ground state indicating a major structural rearrangement following loss of an electron. No signatures of the initially prepared Franck−Condon region or states during the charge transfer process were resolved, presumably due to their short lifetimes.

Peak assignments for the radical cation can be inferred by comparison with DFT calculations. Calculations were performed at the B3LYP/6-31G level on the neutral C343 and neutral C343 bound to a solvated titanium atom, and open-shell DFT at the ub3lyp/6-31G* level for the radical cation. Theoretical frequencies for the radical cation match remarkably well to those observed in the FSRS data. We assign the 1549 $cm^{-1}$ mode to a C═C/C−N stretch. The weak 1205 $cm^{-1}$ mode is assigned to a $CH_2$ rock/C−C stretch with the rocking motion localized to the piperidine ring in line with the conjugated rings. The 1358 $cm^{-1}$ feature, which is small but reproducible in all data sets, is primarily an in-plane hydrogen rocking motion. The calculated structures show a 0.3 Å increase in the C−N bond length as the molecule goes from neutral to the radical cation. This change supports the conclusion from the resonance Raman data that the hole is localized on the carbon backbone, and the single C═C stretching frequency and the increased electron density in the C−N bond indicate that the hole is stabilized over the entire conjugated ring system.

The 1.3 ps decay constant observed in the C═C stretching amplitude has not been reported by previous transient absorption studies. Electron donation from a photoexcited outer sphere dye molecule into $TiO_2$ could account for dynamics on this time scale but should result in a rise, not decay, of the radical cation amplitude. A similar argument exists for the possibility of donation from a

relaxed excited state.[3] Possible explanations for this decay include a fast back electron transfer component, a change in resonance conditions due to solvation, or electron donation to the bound cation from unbound C343. Previous transient absorption experiments which should be sensitive to fast back electron transfer did not reveal changes at this time scale.[22] Experiments performed in $H_2O$ and $CH_3OD$ solvents, which perturb either the dielectric constant or solvent reorientation times, did not result in a conclusive change in the dynamics; however, the vibrational signals in the $H_2O$ experiments were quite small, and the nature of solvation at the nanoparticle interface is unknown. Given the available data at this point, solvation or hole transfer from bound to unbound C343 in our highly concentrated solution are likely explanations for the 1.3 ps decay component.

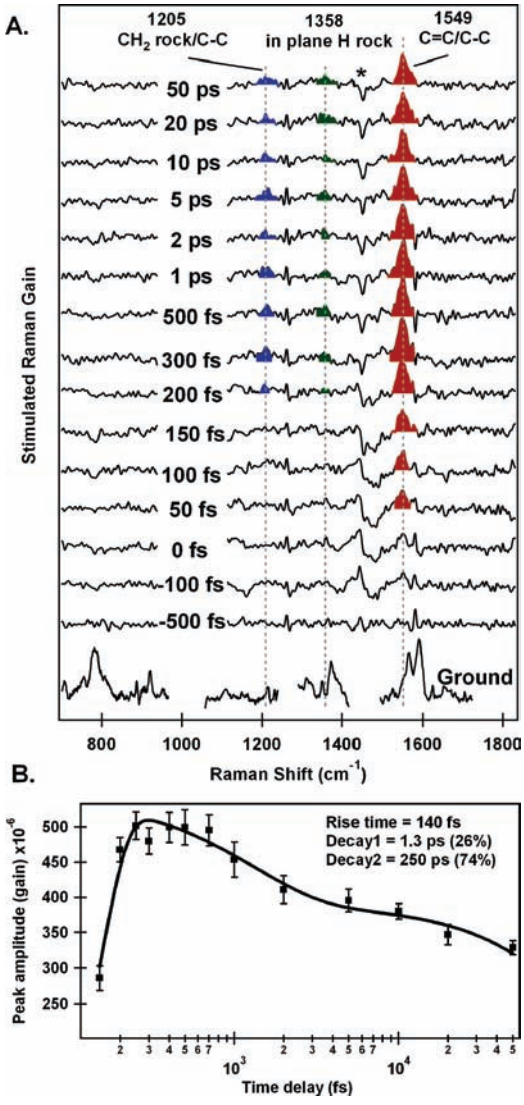


***Figure 3.*** (A) Time-resolved femtosecond stimulated Raman spectra of Coumarin 343 bound to $TiO_2$ nanoparticles, with the neutral ground state spectrum. Excited state peaks at 1205, 1358, and 1549 $cm^{-1}$ grow in with the 120 fs time constant assigned to the formation of the radical coumarin cation. The asterisk represents a solvent artifact. (B) Amplitude of the 1549 $cm^{-1}$ peak fit to two exponentials convoluted with the cross correlation time. Data were obtained with 140 fs time resolution.

The combination of ground and excited state Raman techniques used here indicates that the injected electron comes from the pi backbone structure of Coumarin 343, the donation mechanism involves multiple nuclear coordinates including ring breathing and carbon bond stretching motions, and the delocalized hole resides in the carbon backbone. Additionally, direct binding through the carboxylic acid is verified through the enhancement of local surface Ti−O stretching modes, which indicate significant orbital overlap upon binding.

Coumarin's success as a solar cell sensitizer is limited by the width of its absorption spectrum and the efficiency of unwanted charge recombination. DSSCs made with coumarin derivatives, which increase the conjugated system by introducing linkers in the carboxylic acid foot and methyl groups on the unconjugated rings, as well as adding electron-withdrawing cyano groups near the binding site, have reached solar energy conversion efficiencies of 5.6%,[13] with absorptions extending past 600 nm. However, with the knowledge that the donated electron in the highly efficient Coumarin 343 transfer process comes from the conjugated rings, extending this ring conjugation to phenalene or phenanthrene-like structures to increase the absorption window, while leaving the carboxylic acid/cyano foot unmodified, might result in higher efficiency solar cells with slow recombination times.

**Acknowledgment.** We thank Matthew Sheldon for TEM images. This work was supported by the Mathies Royalty Fund.

**Supporting Information Available:** Complete experimental details, TEM image of $TiO_2$ nanoparticles, resonance Raman spectrum of Coumarin 343 at 508 nm. This material is available free of charge via the Internet at http://pubs.acs.org.

## References

(1) Balzani, V. *Electron Transfer in Chemistry*; Wiley-VCH: Weinheim, 2001; Vol. 1.
(2) Duncan, W. R.; Prezhdo, O. V. *Annu. Rev. Phys. Chem.* **2007**, *58*, 143–184.
(3) Anderson, N. A.; Lian, T. Q. *Annu. Rev. Phys. Chem.* **2005**, *56*, 491–519.
(4) Huber, R.; Moser, J. E.; Gratzel, M.; Wachtveitl, J. *J. Phys. Chem. B* **2002**, *106*, 6494–6499.
(5) Marcus, R. A.; Sutin, N. *BBA* **1985**, *811*, 265–322.
(6) Kukura, P.; McCamant, D. W.; Mathies, R. A. *Annu. Rev. Phys. Chem.* **2007**, 58.
(7) Kukura, P.; McCamant, D. W.; Yoon, S.; Wandschneider, D. B.; Mathies, R. A. *Science* **2005**, *310*, 1006–1009.
(8) Rehm, J. M.; McLendon, G. L.; Nagasawa, Y.; Yoshihara, K.; Moser, J.; Gratzel, M. *J. Phys. Chem.* **1996**, *100*, 9577–9578.
(9) Ghosh, H. N.; Asbury, J. B.; Lian, T. Q. *J. Phys. Chem. B* **1998**, *102*, 6482–6486.
(10) Huber, R.; Moser, J. E.; Gratzel, M.; Wachtveitl, J. *Chem. Phys.* **2002**, *285*, 39–45.
(11) Kondov, I.; Thoss, M.; Wang, H. B. *J. Phys. Chem. A* **2006**, *110*, 1364–1374.
(12) Enea, O.; Moser, J.; Gratzel, M. *J. Electroanal. Chem.* **1989**, *259*, 59–65.
(13) Hara, K.; Sayama, K.; Ohga, Y.; Shinpo, A.; Suga, S.; Arakawa, H. *Chem. Commun.* **2001**, 569–570.
(14) Zhang, X.; Zhang, J. J.; Xia, Y. Y. J. *Photochem. Photobiol., A* **2008**, *194*, 167–172.
(15) Kandavelu, V.; Huang, H. S.; Jian, J. L.; Yang, T. C. K.; Wang, K. L.; Huang, S. T. *Sol. Energy* **2009**, *83*, 574–581.
(16) Myers, A. B. *Chem. Rev.* **1996**, *96*, 911–926.
(17) Doorn, S. K.; Hupp, J. T. *J. Am. Chem. Soc.* **1989**, *111*, 4704–4712.
(18) Shim, S.; Mathies, R. A. *J. Phys. Chem. B* **2008**, *112*, 4826–4832.
(19) Frisch, M. J.; et al. *Gaussian 03*; Gaussian Inc.: Wallingford, CT, 2004.
(20) Nomoto, T.; Onishi, H. *Chem. Phys. Lett.* **2008**, *455*, 343–347.
(21) McCamant, D. W.; Kukura, P.; Yoon, S.; Mathies, R. A. *Rev. Sci. Instrum.* **2004**, *75*, 4971–4980.
(22) Ghosh, H. N. *J. Phys. Chem. B* **1999**, *103*, 10382–10387.

JA907188B